

XAFS experiments at beamline I811, MAX-lab synchrotron source, Sweden

Stefan Carlson,* Maria Clausén, Lidia Gridneva, Bengt Sommarin and Christer Svensson

MAX-lab, Lund University, PO Box 118, SE-22100 Lund, Sweden.

E-mail: stefan.carlson@maxlab.lu.se

A description of a new facility for X-ray absorption spectroscopy at the materials science beamline, I811, at MAX-lab synchrotron source, Lund, Sweden, is given. The beamline is based on a superconducting multipole wiggler source inserted in a straight section of the 1.5 GeV MAX-II ring. X-rays in the energy range 2.4–12 keV are extracted by a standard optical scheme consisting of a vertical collimating first mirror, double-crystal monochromator, and a second vertically focusing mirror. The second monochromator crystal provides sagittal focusing. The total flux impinging on the sample at 9 keV is 5×10^{11} photons s^{-1} , for a minimum beam spot of 0.5 mm \times 0.5 mm. The beamline has facilities for experiments in transmission, fluorescence and total-electron-yield mode and experiments have been performed by international research groups on a wide range of materials, such as dilute systems with metal concentrations below 10 p.p.m.

Keywords: X-ray absorption spectroscopy; XAFS; XANES; EXAFS; materials science.

1. Introduction

A new beamline, I811, based on a superconducting multipole wiggler source has been constructed at MAX-lab synchrotron source, Lund, Sweden. The wiggler is inserted in the MAX-II storage ring, which is a medium-sized (90 m circumference) third-generation synchrotron operated at 250 mA. The beamline is designed for materials science X-ray diffraction and spectroscopy experiments in the energy range 2.4–20 keV (5–0.6 Å).

The MAX-II storage ring has previously been used for experiments mainly in the soft X-ray region, but the development of new superconducting wigglers made it possible to obtain higher flux and to shift the critical energy to around 5 keV. It was then decided to construct a beamline dedicated to materials science research. This beamline would be used to obtain X-ray absorption fine structure (XAFS), surface and bulk diffraction data from specimens in air or special sample environments (*e.g.* cryostat, furnace, pressure cell). The optical concept of the beamline was developed by M. Grehk and P. O. Nilsson and has previously been reported (Grehk & Nilsson, 1999, 2001). For an example of a similar beamline concept, the report by Patterson *et al.* (2005) on the materials science beamline at the Swiss Light source (SLS) is recommended.

We describe here the optical layout and performance of the beamline. Furthermore, the facilities for XAFS experiments and some preliminary experimental results are described.

2. X-ray source and beamline

2.1. Superconducting wiggler X-ray source

As mentioned above, the X-ray source (LeBlanc *et al.*, 2000) is a liquid-He-cooled superconducting multipole wiggler. It is 1.5 m long with 49 poles and has a 65 mm period. The maximum magnetic field is 3.5 T at an applied current on the magnets of 200 A. The critical energy is $E_c = 5$ keV and the wiggler deviation parameter $K = 20$. It radiates a total power of 5 kW. At 10 keV the wiggler emits approximately 2×10^{15} photons s^{-1} (0.1% bandwidth) $^{-1}$ with horizontal and vertical FWHM of 7 mrad and 0.3 mrad, respectively. The superconducting magnets are housed within a 400 l cryostat that is regularly topped up with He. Full specifications and properties of beamline I811 are given in Table 1.

2.2. Front-end layout

The first part of the beamline (the front-end) is situated within the bremsstrahlung radiation shield that surrounds the storage ring. Approximately 40% of the wiggler beam is allowed into the beamline by a water-cooled copper aperture (60 mm \times 40 mm). The beam is secured within the front-end by three water-cooled copper heat absorbers, each with a UHV valve behind, and a lead synchrotron radiation shutter. A fast UHV valve, with a closing time of less than 0.5 s, is also installed to protect the storage ring. The shape of the beam is controlled by a water-cooled primary slit system, equipped with motorized horizontal and vertical molybdenum blades.

Table 1
Beamline I811 specifications and properties.

Ring current	250 mA
Source	Superconducting wiggler
Magnetic field	3.5 T
Magnet period	65 mm
Number of poles	49
Wiggler K value	20
Source flux	2×10^{15} photons s^{-1} (0.1% bandwidth) $^{-1}$ (calculated)
Source size	50 $\mu\text{m} \times 250 \mu\text{m}$ ($v \times h$)
Source divergence	0.3 mrad \times 6.0 mrad ($v \times h$)
Front-end slits	6.4 m from source
Mirror 1	10 m from source, pitch 3–10 mrad
Monochromator	18 m from source, $\Delta E/E = 2 \times 10^{-4}$
Mirror 2	20 m from source, pitch 3–10 mrad
Flux at sample	5×10^{11} photons s^{-1} (0.02% bandwidth) $^{-1}$ at 9 keV (measured)
Beam size at sample	Typically 0.5 mm \times 1.0 mm ($v \times h$)

To remove low-energy photons, a 12 μm -thick carbon filter that absorbs a power of about 700 W intercepts the beam before the primary slit system. The radiation power leaving the front-end and entering the rest of the beamline is estimated to be 2.2 kW (Grehk & Nilsson, 1999).

2.3. Mirrors and monochromator

The optical layout of the beamline is fairly conventional and is shown schematically in Fig. 1. The first mirror is placed 10 m from the wiggler and provides vertical collimation as well as the removal of higher-order harmonics. The mirror was manufactured by Zeiss/Bestec and consists of a silicon blank with 200 \AA Rh coating (K edge: 23 keV). It has an optically active length and width of 1000 mm and 60 mm, respectively. The pitch range is 3–10 mrad and the cylindrical bending radius can be varied between 2000 and 6000 m. The surface of the mirror is polished to an r.m.s. roughness of less than 2 \AA , and r.m.s. residual meridional and sagittal slope errors are less than 2.4 μrad and 9.7 μrad . The mirror is water-cooled on its sides and is operated under UHV conditions. The maximum absorbed heat load in the mirror is estimated to be 900 W. The contribution from L edges due to the Rh mirror coating (3–3.4 keV) may have an impact on the XAFS signal at the Cl and Ar K edges and for the L edges of Tc, Ru, Rh, Pd and Ag. No systematic measurements of the effect on the XAFS signal by the Rh coating have yet been made, but measurements on the Cl K edge of NaCl did not show any noticeable features that could be derived from interference by Rh L -edge absorption. In cases when the first mirror is not used, a fixed 100 μm -thick carbon filter before the monochromator absorbs a corresponding amount of heat. Its holder allows the passage of a mirrored beam below the filter. Furthermore, three movable carbon filters (1.0, 0.3 and 0.1 mm thick) have been installed to provide the possibility of attenuating the beam before it hits the first monochromator crystal.

The second Zeiss/Bestec mirror is placed 20 m after the wiggler and is similar in design to the first mirror, but is constructed using Zerodur instead of silicon. The optically active length and width is 1000 mm and 80 mm, respectively. The variable cylindrical curvature of 800–5300 m permits

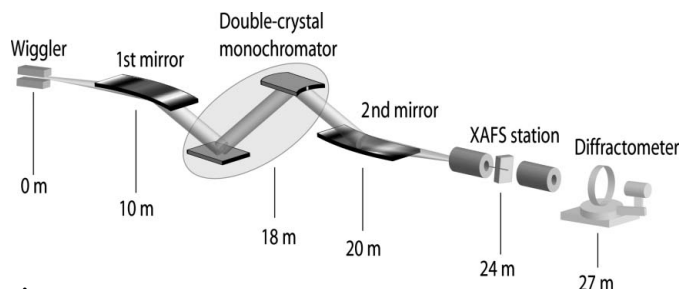


Figure 1
The basic optical concept of beamline I811. The first mirror collimates the wiggler beam vertically before a double-crystal monochromator (DCM), and the second mirror refocuses the beam to the sample position. The second DCM crystal provides sagittal (horizontal) focusing.

vertical focusing at the experimental stations (22–27 m from source). Since such focusing introduces a vertical divergence that may be undesirable in high-resolution diffraction experiments, the user may choose to use the mirror in a plane geometry.

The double-crystal monochromator (DCM), manufactured by Accel GmbH, consists of a pair of crystals that can be precisely positioned and oriented in the X-ray beam. The energy range 2.4–20 keV can be covered using interchangeable pairs of Si(111) and Si(311) crystals. At present, only Si(111) crystals are available, which reduce the operating energy range to 2.4–12 keV. Two successive Bragg reflections, with an inherent energy resolution (given by the Darwin angular width) of 0.014% directs photons of the desired energy parallel to the incoming beam direction, but offset upward by 25 mm. This ‘fixed exit’ operation is achieved by placing both crystals on a common rotation stage with the diffracting surface of the first crystal on the rotation axis, and translating the second crystal along two perpendicular directions within the scattering plane. When tilting the beam with the first mirror, the positions of the monochromator crystals and goniometer angle are adjusted, and the second mirror is tilted and placed at the 25 mm offset position. Currently, the monochromator is operated without any encoders. For this reason, reference foils are used in each measurement to obtain a reliable energy scale. An upgrade with encoder on the Bragg-angle rotation stage is being pursued.

Additional degrees of freedom allow corrections for crystal yaw, roll and pitch. The change of pitch can be made on both crystals using piezo-electric actuators. These are used when performing so-called detuning to remove higher-order harmonics, *i.e.* one of the crystals is slightly rotated out from the perfect Bragg position to avoid the undesirable higher-order reflection. The piezo actuators can also be used for fast scan operation (piezo-scan mode), where the actuators on both monochromator crystals are moved simultaneously so that short XANES scans are obtained. A time resolution below 10 ms using this technique has been reported (Bornebusch *et al.*, 1999). The piezo-scan option is currently not available, but commissioning of it is expected in the near future. The large heat load absorbed by the first DCM crystal is removed by indirect water cooling and the remaining distortion of the crystal shape is corrected by a ‘Torii’ bending

mechanism (Schulte-Schrepping *et al.*, 1995). The second crystal provides sagittal focusing by cylindrical bending of a ribbed crystal to a variable curvature radius ($R_{\min} = 1$ m) in a flexure-hinge fixture developed at the ESRF (Freund *et al.*, 1998). The DCM is operated in a 10^{-5} Pa vacuum.

2.4. Beam-position monitors

For optimization of the white-beam properties, three beam-position monitors (BPMs) are installed in the beamline. The first BPM is a water-cooled copper plate that is coated with fluorescent material and inclined 45° with respect to the beam to allow an image to be observed by a video camera perpendicular to the beam. It is placed after the first mirror and moved pneumatically in and out of the beam. The second BPM is placed at the entrance of the monochromator and measures the photo-induced current in a tantalum wire (250 μm thick) that is translated vertically through the beam. A third BPM measures the photo-induced currents from the monochromatic beam in one of the molybdenum vertical slit blades installed directly after the monochromator crystals.

3. Experimental stations

3.1. Experiment hutch

The experimental hutch is 5.6 m \times 8.9 m and is designed to accommodate an experimental table for XAFS and general X-ray diffraction equipment, as well as a large surface diffractometer. The height is 5 m, with a crane (capacity 1250 kg) leaving about 4 m effective height inside the hutch. The walls and ceiling are made of 6 mm-thick steel, calculated to stop all X-ray radiation energies that the wiggler can emit. A 3 m-wide sliding door in the back of the hutch allows large experiment equipment to be inserted into the hutch, and in direct proximity to the control room a normal door for easy access is available. An air-conditioning system has been installed, providing a temperature stability of $\pm 1^\circ$. For user experiments a separate purified air system as well as a normal water supply is available. Other gases, such as nitrogen, can be obtained from bottles used at the XAFS station. Cable chicanes for permanent and user installations are available in the hutch walls. In addition, a general-purpose patch panel with motor connectors and signal inputs/outputs is mounted close to the experiment table and connects to the control-room electronics. The control room has space for four or five people and is built adjacent to the experiment hutch. A lead-glass window has been installed for visual observation of the experiment and facilities for surveillance by video cameras are available. The control room houses all control electronics and motor drivers for the beamline, as well as computers for experiment and beamline control, as well as for data analysis. A complete laboratory for XAFS sample preparation is currently being built in close proximity to the beamline. It includes a fully featured glove box, ultra-pure water system, ultracentrifuge, pellet press, fume cupboards, analytical balance and other laboratory equipment.

3.2. XAFS station

The XAFS station is based on a 0.9 m \times 1.8 m optical table constructed for a load of at least 100 kg. On the table, a system with horizontal and vertical slits (mentioned above) defines the size of the beam. XAFS data from the sample and reference sample can be collected in transmission and fluorescence yield modes.

For transmission XAFS, three IC-Spec ionization chambers (Oxford-Danfysik) are used. The ionization chambers are operated with fixed gas mixtures for optimum absorption at various energies. The maximum pressure sustained by each chamber is 2×10^5 Pa. A gas system with He, N₂, Ar and Kr is connected to the ion chambers for optimum gas pressures and flow. A power supply (ISEG Spezialelektronik GmbH, VHQ103M) feeds the ion chambers with a maximum voltage of 3 kV. In normal operation around 2 kV is sufficient. The ion-chamber signals are measured by Keithley 428 current amplifiers and the amplified signals are read by a 16 bit analog-to-digital converter (Hytec Electronics, MADC 2508).

The fluorescence yield from the sample can be measured using a five-grid ion-chamber Lytle detector (The EXAFS Company), or with an energy-dispersive solid-state silicon-drift detector (Vortex 90-EX, SII Nano Technology USA). For fluorescence measurements of metal concentrations around and above 1000 p.p.m., the large solid angle of the Lytle detector is preferable, but for lower concentrations the Vortex detector is a better option. The Vortex detector has a 50 mm² active area in a single element, and combined with digital pulse-processing electronics (XIA, LLC) a maximum output count rate of 3×10^5 counts s⁻¹ (0.25 μs peaking time) without pile-up problems can be achieved. The resolution at the highest count rate is about 250 eV. At 1×10^5 counts s⁻¹ (1 μs peaking time) the resolution is improved to about 140 eV. It has been used for detection and XAFS measurements of p.p.m. concentrations of *e.g.* Mn-, Fe- and Cu-containing impurities in paper fibres (Camerani *et al.*, 2005).

The sample stage consists of computer-controlled vertical and horizontal translations with micrometre precision, as well as a goniometer for tilting the sample ($\pm 17^\circ$) along the X-ray beam. A small goniometer is also available for 360° rotation of the sample in the beam. In both transmission and fluorescence mode the sample is mounted in the Lytle detector sample holder. This allows the use of *e.g.* a helium atmosphere around the sample, which is necessary for experiments at low energies due to the X-ray absorption by air. For non-ambient sample conditions, a cryostat/furnace (100–770 K) can be attached to the Lytle detector or used in transmission mode. A closed-cycle cryostat (Janis Research Company), operating with the sample in a vacuum, is available for sample temperatures down to 10 K.

3.3. Surface diffraction station

Beamline I811 has a fully featured surface science diffractometer. It has not yet been commissioned and used in experiments, and a full description of the system is out of scope for this report. The diffractometer was manufactured by

Newport/Micro-control and allows a small removable ‘baby’ process chamber, weighing up 20 kg, to be mounted with the sample surface in any orientation. In addition, it is possible to support a large 500 kg UHV system on a horizontal rotation table. A full report on the diffractometer system will be given in a subsequent paper.

3.4. Beamline control systems

The control system is divided into two parts. Firstly, the PLC-system that controls the beamline vacuum equipment and safety system; this system is common to all MAX-lab beamlines and has a user-friendly graphical interface. Secondly, the control of all stepper and DC motors, as well as data collection, is performed by a control system based on the software *SPEC* (Certified Scientific Software); *SPEC* communicates with the different stepper and DC motors controllers *via* different communication protocols, such as VME, GPIB, RS232 and TCP/IP.

To simplify for the users, a graphical user interface (GUI) developed using Tcl/Tk has been implemented to control *SPEC*. This GUI can be used from any computer at the beamline with MS Windows operating system. The user can choose to download the GUI to their own computers to obtain experiment control, or use one of the available computers in the control room. The GUI provides facilities for X-ray beam optimization, detector set-up and sample manipulation, as well as control over three XAFS data-collection modes: continuous-, step- and piezo-scan. It is flexible enough to allow complex automatic data-collection series over extended periods with *e.g.* sample manipulation in between scans. The data file format for XAFS that is supported at beamline I811 is based on ASCII-text files with columns of energy, detector data and absorption factor. Each column with detector data is automatically corrected for electronic noise (dark current). At the top of each data file a small number of experiment parameters and user comments are written. Both *SPEC* and the GUI produce log files for a more comprehensive trace of actions backwards in time.

4. Experimental results

In spring 2004 the first XAFS user experiments were performed at beamline I811, and a continuous development of the XAFS station has been undertaken. In this section, results from recent XAFS experiments are described. Data for Figs. 2–6 were analyzed and plotted using the software *Athena* (Ravel & Newville, 2005).

4.1. XAFS experiments

To illustrate the performance of the XAFS station, measurements on a copper-foil standard and sodium thio-sulfate are presented. Copper metal is probably the best characterized standard for XAFS experiments. A transmission measurement over the Cu *K* edge and the corresponding k^3 -weighted χ plot are shown in Figs. 2 and 3, respectively. The clearly visible pre-edge feature in the Cu spectrum at 8900 eV

(Fig. 4) indicates that the resolution is better than 2 eV, which is close to the intrinsic resolution of Si(111) monochromator crystals (approximately 1.4 eV) and is sufficient for near-edge studies. It can be seen from the χ plot (Fig. 3) that reasonable data quality extends out to a k value of 15–16 Å⁻¹.

Sodium thiosulfate was included here to show the possibilities at beamline I811 of performing XAFS experiments at the sulfur *K* edge. This is experimentally very demanding due to

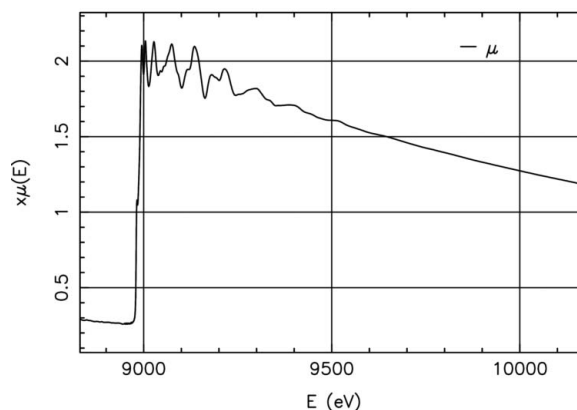


Figure 2 X-ray absorption spectrum collected from a 7 μm-thick Cu metal reference foil.

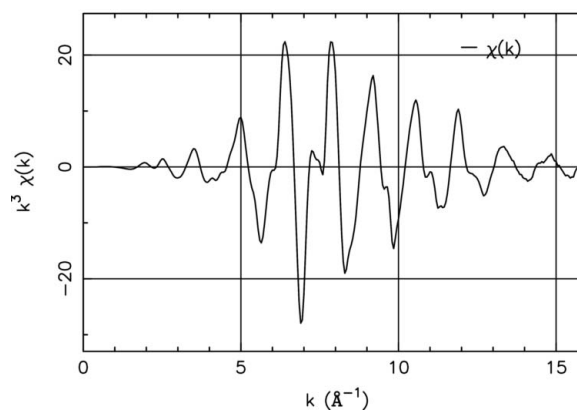


Figure 3 χ -data, k^3 -weighted, from the Cu foil measurement.

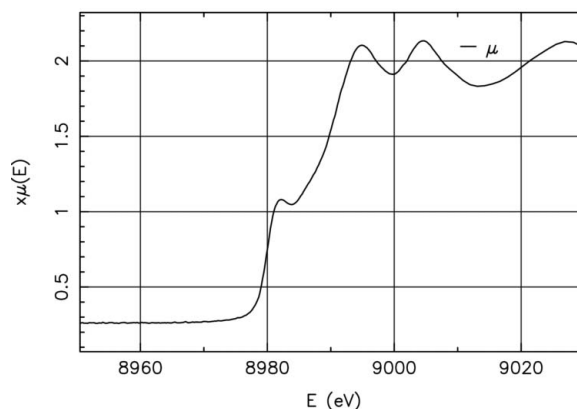


Figure 4 XANES measurement over the Cu *K* edge, showing a resolved pre-edge feature that implies an energy resolution better than 2 eV.

the high attenuation of the X-ray beam through beamline windows and beam paths. The beamline has a number of installed windows: a 12 μm -thick carbon filter in the front-end, a 13 μm -thick Mylar film after the monochromator and a 250 μm -thick beryllium window at the end of the beamline. For an experiment in fluorescence mode, two additional 25 μm Kapton windows in the I_0 ion chamber also contribute to the absorption. At 2500 eV, these windows attenuate the beam by 50%. Fig. 5 shows the recorded spectrum from sodium thiosulfate, prepared by Sandström & Persson (2005). In this case the X-ray mirrors were not set up to provide proper harmonic rejection; instead the second monochromator crystal was tilted out of perfect alignment so that 30% of the maximum intensity remained (detuned by 70%). A 60 s continuous scan was performed with the sodium thiosulfate powder mounted on a sulfur-free Mylar tape in the Lytle detector. Helium was used in the I_0 ion chamber as well as purged through the beam path and sample chamber, to reduce attenuation of the primary beam and scattered radiation.

Finally, in Fig. 6 we show an example of a highly sensitive measurement on iron-containing particles on paper fibres (Camerani *et al.*, 2005). The Fe content has previously been

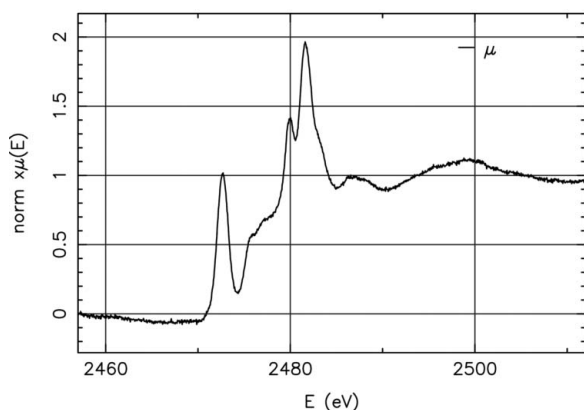


Figure 5
Sodium thiosulfate, $\text{Na}_2\text{S}_2\text{O}_3$, XANES from a thin powder sample on a Mylar film. The spectrum was collected in fluorescence mode by a continuous quick-XAFS scan with total exposure time of 60 s.

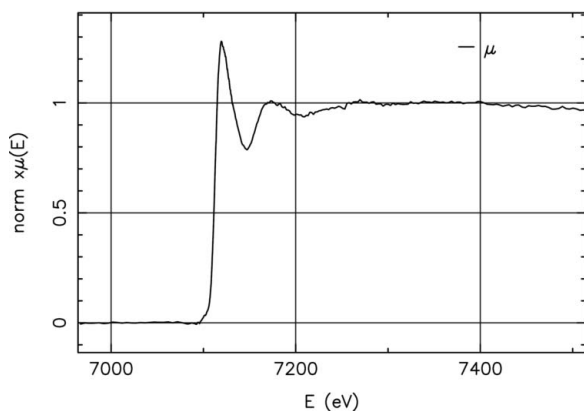


Figure 6
XAFS measurement over the Fe K edge on a paper fibre sample with 9 p.p.m. iron concentration.

determined by chemical analysis to be 9 p.p.m. The Vortex fluorescence detector was placed a few centimetres from the sample, perpendicular to the incoming beam path in the horizontal plane. A Mn filter before the detector was used to remove some of the background signal below the Fe K fluorescence peak. The flux on the 1 mm \times 1 mm beam spot hitting the sample was approximately 10^{11} photons s^{-1} . A throughput of about 1×10^5 counts s^{-1} was obtained (1 μs peaking time) in a 1–10 keV range, and the part constituting the iron K-edge signal was 5000–10000 counts s^{-1} (200 eV energy window).

4.2. Conclusions and future prospects

Beamline I811 provides the XAFS user community with the facilities to perform experiments in a large number of different research fields. The high flux, low beam divergence and spectral purity, combined with high-quality detectors and electronics, give a high signal-to-noise ratio which can be used in accurate structural investigations and measurements on low metal concentrations. In the coming few years, further development of the XAFS station is planned. To increase the sensitivity of fluorescence measurements for *e.g.* experiments on proteins, a multi-element Ge or Si(Li) detector will be purchased, and techniques using HOPG crystals (Pease *et al.*, 2001) as narrow energy filters will be pursued. Finally, means of focusing the beam by *e.g.* X-ray mirrors in Kirkpatrick–Baez geometry will be developed for microbeam X-ray fluorescence and XAFS experiments, important in mapping of metal distribution in materials as well as giving the possibility for high-pressure XAFS research using diamond-anvil cells.

This work was supported by the Swedish Research Council and Knut och Alice Wallenbergs Stiftelse. Additional support was granted by Craafordska Stiftelsen and The Faculty of Science and Technology, Norwegian University of Science and Technology. Crucial help has been provided by the MAX-lab technical staff. Special thanks to Caterina Camerani, Carina Johansson and Stuart Ansell for providing the spectrum in Fig. 6, and to Professor Ingmar Persson and Professor Magnus Sandström for invaluable help in developing the XAFS station.

References

- Bornebusch, H., Clausen, B. S., Steffensen, G., Ützenkirchen-Hecht, D. L. & Frahm, R. (1999). *J. Synchrotron Rad.* **6**, 209–211.
- Camerani, C., Johansson, C. & Ansell, S. (2005). Experiment No. I811-034. MAX-Lab, Lund, Sweden.
- Freund, A. K., Comin, F., Hazemann, J.-L., Hustache, R., Jenninger, B., Lieb, K. & Pierre, M. (1998). *Proc. SPIE*, **3448**, 144–155.
- Grehk, T. M. & Nilsson, P. O. (1999). *MAX-Lab Activity Report 1998*, edited by J. N. Andersen, R. Nyholm, S. L. Sorensen and H. Ullman, Vol. 260–261. MAX-Lab, Lund, Sweden.
- Grehk, T. M. & Nilsson, P. O. (2001). *Nucl. Instrum. Methods Phys. Res. A*, **467–468**, 635–638.

- LeBlanc, G., Wallén, E. & Eriksson, M. (2000). *MAX-Lab Activity Report 1999*, edited by J. N. Andersen, R. Nyholm, S. L. Sorensen and H. Ullman, Vol. 45–47. MAX-Lab, Lund, Sweden.
- Patterson, B. D., Abela, R., Auderset, H., Chen, Q., Fauth, F., Gozzo, F., Ingold, G., Kühne, H., Lange, M., Maden, D., Meister, D., Pattison, P., Schmidt, Th., Schmitt, B., Schultze-Briese, C., Shi, M., Stampanoni, M. & Willmott, P. R. (2005). *Nucl. Instrum. Methods Phys. Res. A*, **540**, 42–67.
- Pease, D. M., Budnick, Daniel, J. I., Taylor, B., Frenkel, A., Pandya, K., Grigorieva, I. K. & Antonov, A. A. (2001). *J. Synchrotron Rad.* **8**, 336–338.
- Ravel, B. & Newville, M. (2005). *J. Synchrotron Rad.* **12**, 537–541.
- Sandström, M. & Persson, I. (2005). Experiment No. I811-045. MAX-Lab, Lund, Sweden.
- Schulte-Schrepping, H., Materlik, G., Heuer, J. & Teichman, T. (1995). *Rev. Sci. Instrum.* **66**, 2217–2219.